



Interest of metabonomic approach in environmental nephrotoxics: Application to aristolochic acid exposure



M. Duquesne^{a, c}, A.-E. Declèves^{b, c}, E. De Prez^d, J. Nortier^d, J.M. Colet^{a, c, *}

^a Department of Human Biology & Toxicology, Faculty of Medicine, University of Mons, Mons, Belgium

^b Laboratory of Molecular Biology, Faculty of Medicine, Mons, Belgium

^c Research Institute for Health Sciences and Technology, University of Mons, Mons, Belgium

^d Laboratory of Nephrology, Faculty of Medicine, University Libre de Bruxelles, Brussels, Belgium

ARTICLE INFO

Article history:

Received 13 April 2017

Received in revised form

23 June 2017

Accepted 6 July 2017

Available online 8 July 2017

1. Introduction

In 1993, the occurrence of a rapidly progressive form of renal interstitial fibrosis associated with a weight loss diet which included the ingestion of pulverized plant extracts used in traditional Chinese medicine, led to the description of a new toxic nephropathy (Vanherweghem et al., 1993). The identification of aristolochic acids (AA) in these powders brought to attention the severe toxicity of certain species of *Aristolochia* (Vanhaelen et al., 1994). Ever since, secondary nephropathies resulting from the toxicity of plants containing AA have been described worldwide (Debelle et al., 2008). The similarity between the histological aspects of this particular nephropathy and the so-called Balkan endemic nephropathy (BEN) (Grollman et al., 2007), combined with the association between these types of renal disease and urinary tract cancers (Cosyns et al., 1999; Nortier et al., 2000), proved instrumental in reviving an old hypothesis on the aetiology of BEN. In 1969, Ivic had suggested that the latter, occurring in certain villages throughout the Danube Valley, might be caused by the chronic ingestion of the seeds of the *Aristolochia clematis*, a

common plant growing in the wheat fields of these endemic regions (Ivic, 1969). This hypothesis has now been confirmed by the discovery of specific DNA adducts that are formed by the metabolites of AA in the renal tissue and the urothelial tumours of those patients suffering from BEN (Jelakovic et al., 2012).

Today, the term “aristolochic acid nephropathy” AAN is used to include any form of toxic interstitial nephropathy that is caused either by the ingestion of plants containing AA as part of traditional phytotherapies (e.g. Chinese medicine (Commission of the Ministry of Public Health, 2000; IARC, 2002), Japanese Kampo (Takako et al., 2002) and Ayurvedic medicine), or by the environmental contaminants in food (BEN) (Cosyns et al., 1994; Grollman et al., 2007). Although, initially, the Belgian cohort only included over 100 patients, it is estimated that exposure to AA affects 100,000 people in the Balkans (where the total number of patients with kidney disease amounts to approximately 25,000), 8,000,000 people in Taiwan and more than 100,000,000 in mainland China (Yang et al., 2011; Chen et al., 2012). Given the fact that the nephrotoxic effect of AA is irreversible and that their carcinogenic effects may be very slow in manifesting themselves after the patient's initial exposure, AAN and associated cancers are likely to become a major public health issue in the years to come (Gökmen et al., 2013).

Aristolochic acid nephropathy has been successfully reproduced in various experimental models. Both experimental and clinical studies indicate that the proximal tubule, particularly in its straight part (S3), is targeted by AA (Debelle et al., 2002; Lebeau et al., 2005). In 2002, Debelle et al., showed that a daily subcutaneous injection of 10 mg/kg of AA mixture (40% AAI; 60% AAI) in salt-depleted rats induced an interstitial fibrosis and renal failure within 35 days. Using the same protocol, Lebeau et al., collected urine samples to demonstrate a correlation between structural and functional injuries of the proximal tubule (increased urinary excretion rates of brush border enzymes and altered reabsorption capacity of microproteins by endocytosis). Two phases were finally observed: a first one, characterized by a transient proximal tubular necrosis (maximal at day 5), followed by an interstitial inflammation making the link with the second phase, characterized by the onset of severe tubular atrophy interstitial fibrosis (from day 7 to day 35).

Abbreviations: AA, aristolochic acid; AAI, aristolochic acid I; AAI, aristolochic acid II; AAI+AAII, mixture of aristolochic acid I and II; AAN, aristolochic acid nephropathy; BUN, blood urea nitrogen; GLUT, glucose transporter; OAT, organic anion transporter; OSOM, outer stripe of outer medulla; PTEC, proximal tubule epithelium cell; rOAT, rat organic anion transporter; SCR, serum creatinine; SGLT, sodium-glucose transporter; WRS, Wilcoxon rank-sum test.

* Corresponding author. Dept of Human Biology & Toxicology, University of Mons, 20 place du Parc, 7000 Mons, Belgium.

E-mail address: jean-marie.colet@umons.ac.be (J.M. Colet).

Although mechanistically informative, the conventional markers used in those previous studies lacked of sensitivity. When abnormal levels of those markers are noticed, it is usually too late because irreversible damages are already reached. More recently, several authors published encouraging results showing that the metabolomic investigation of urines from animals exposed to nephrotoxicants, including AAs, was able to detect renal injuries at very early stages, also making possible some inferences in the drug-targeted biochemical pathways (Hu et al., 2017; Zhao et al., 2015a). Strategically, urine is the ideal biological fluid to discover biomarkers for renal pathologies as it is the case for AA intoxication. It can be easily and noninvasively collected in almost all patients and is well suited for kinetics studies. However, the major difficulty in using urine as an experimental matrix is the wide variability among individuals (Rucevic et al., 2012). Nevertheless, changes in the relative levels of dozens of urine metabolites may provide precious clues on cellular mechanisms responsible for damages caused to the kidneys (Wishart, 2006). This is the basis of the metabolomic approach, defined as a high speed measurement of a large quantity of low MW molecules (<1500 Da), the metabolites, present in cells, tissues and organs. The spectrometric analysis of biofluids allows the identification and quantification of dozens of metabolites in a few minutes. Discriminant metabolites identified are then related to biochemical pathways and specific biological processes.

Using this predictive omic tool, we revisited our rat models of AAs intoxication to identify early urinary biomarkers which could be further developed for a quick and a noninvasive detection of renal injuries caused by AA. The predictive aspect is of paramount importance to support patients before the onset of irreversible kidney damage.

2. Material & method

2.1. Chemicals and reagents

AAI (A5512-100 mg, Sigma-Aldrich Chemie GmbH, Germany), AAI (A3774, AppliChem, GmbH, Germany) and mixture of AAI+AAII (40:60) (Acros Organics Co., Geel, Belgium) were dissolved with polyethyleneglycol (PEG400, Fluka Chemie, Buchs, Switzerland) in a stock solution of 20 mg/ml.

2.2. Ethics statement

All experimental protocols were approved by the Animal Ethics Committee of UMONS. Animal care and use were conducted in compliance with the National Institutes of Health (NIH) guidelines for the Care and Use of Laboratory Animals. All invasive practices (subcutaneous injections, blood collections, euthanasia) were performed under isoflurane anesthesia.

2.3. Studies design & animal groups

For each study, rats (aged 4 week-old; weighting 125–150 g; supplied by Elevage Janvier (Le Genest-Saint-Isle, France)) were

housed in the animal care facility within rooms kept at a controlled humidity level between 40 and 60% and a mean temperature of 21 ± 2 °C, with a 12/12-h light/dark cycle. During the quarantine week, animals had free access to standard diet (ref: 11576814, Carfil Quality, Oud-Turnhout, Belgium) and water ad libitum.

The first pilot study was designed to test several doses of the AAI and AAI+AAII. 8 Wistar Han male rats were randomly divided in three groups according to the administered substance: Group AAI (n = 3), group AAI/AAII (n = 3) and control group (n = 2) (see Table 1). Three doses were tested in this pilot study for each toxin (50, 75 or 100 mg/kg) according to a 96-h protocol (described below). In the second study, 18 Wistar Han male rats were randomly divided according to the same previous three groups: AAI 100 mg/kg (n = 6), AAI/AAII 75 mg/kg (n = 6) and control (n = 6). Compared to the pilot study, the exposure was prolonged to 192 h (see protocol description below). Finally, in the third study, AAI toxicity was investigated following the same 96-h protocol as used in the pilot study. 12 Wistar Han male rats were randomly divided in three new groups: One control group (n = 4) and two AAI groups according to the exposed dose: 75 mg/kg (n = 4) or 100 mg/kg (n = 4). Note that the lower dose (50 mg/kg) was not been evaluated for AAI due to the lack of significant effect at this dose for both AAI and the mixture during the pilot study.

2.4. Drugs administration

After one week of acclimatization, rats were randomly allocated to the experimental groups and individually placed in metabolic cages with free access to water and 30–35 g of standard diet daily during 3 days prior to dosing. Drug administration was performed on anesthetized animals. Rats were firstly placed in an induction chamber filled with 4.0% isoflurane (lot number 37003XN, Alcyon, Villers-le-Bouillet, Belgium) at a flow rate of 1.0 l/min, then anesthesia was maintained with 1.5% isoflurane during drug administration. The AAI, AAI/AAII and AAI powders, dissolved in PEG400 (20 mg/ml), were diluted in NaCl 0.9% (50:50) before subcutaneous injection. In the control group, rats were just anesthetized without any other treatment. After dosing, rats were placed back to their metabolic cages and their body weights as well as diet and water consumptions were recorded daily throughout the study duration.

2.5. Protocols & samples collection

2.5.1. Urine samples

Urine samples were collected by fractions of 12 h-periods from the pretest days until end of study. During the collection periods, tubes were placed in refrigerated racks (4 °C) and 500 µl of a solution of 1.0% sodium azide (S8032-25 g, lot number BCBD9551V, Sigma-Aldrich Chemie GmbH, Germany) were previously added in order to avoid bacterial contamination.

In the 192-h protocol, urine samples were also collected by fractions of 12 h from pretest days up to 96 h. Then, urine collection was stopped during 48 h and resumed until the end of study.

Table 1
Summary of the experimental protocols conducted in rats.

	AAI	AAI+AAII	AAII	Control	Timing
Pilot study	50 mg/kg (n = 1) 75 mg/kg (n = 1) 100 mg/kg (n = 1)	50 mg/kg (n = 1) 75 mg/kg (n = 1) 100 mg/kg (n = 1)	X	n = 2	96 h
Second study	100 mg/kg (n = 6)	75 mg/kg (n = 6)	X	n = 6	192 h
Third study	X	X	75 mg/kg (n = 4) 100 mg/kg (n = 4)	n = 4	96 h

2.5.2. Blood samples

600 µl of blood were collected under isoflurane anesthesia from the tail vein, and left during 45–60 min at room temperature. Serum samples were then obtained by centrifugation (15min, 3000 g, 15 min) and stored at –20 °C before analysis into Eppendorf tubes.

Blood samples were collected 24 h before and after dosing, and before euthanasia at either 96 or 192-h post-dose depending on the study groups.

2.5.3. Kidney histology

At the end of the study, anesthetized rats were euthanized by intravenous injection of Nembutal (Ceva Santé Animale, Brussels). Kidneys were decapsulated, blotted dry, and weighted. After longitudinal section, the left kidney was immersed in Duboscq-Brazil fluid (formalin/acetic acid/ethanol containing 1% picric acid/water, 260:70:425:245 vol ratio) for 48 h at room temperature. The fixed samples were thereafter rinsed in 70° ethanol, progressively dehydrated in graded ethanol and butanol baths, and embedded in Paraplast Plus® paraffin according to standard procedures. Paraffin sections of 4–5 µm thickness were cut on a Reichert Autocut 2040 microtome (Reichert Jung, Nossloch, Germany) and mounted on silane-coated glass slides for histological examination. Kidney paraffin sections were stained with Periodic Acid Schiff (PAS), hemalun, and Luxol fast blue to allow the identification of histological structures.

2.6. Clinical chemistry

Serum samples were analyzed for clinical chemistry on an automatic biochemical analyzer (Spotchem EZ SP-4430, Menarini Diagnostics). SPOTCHEM II Kidney-2 kit (lot number QN2J89) was used to measure total protein, albumin, blood urea nitrogen (BUN), creatinine and uric acid.

2.7. Preparation and ¹H NMR spectroscopy analysis of samples

2.7.1. Urine samples ¹H NMR preparation

After centrifugation (5min, 5,000×g at 4 °C), 400 µl of the supernatant fraction were removed to microcentrifuge tubes and 200 µl of 0.2 M sodium phosphate buffer (0.04M NaH₂PO₄+ 0.2 M NaHPO₄, pH 7.0) prepared in 80/20 H₂/D₂O were added to maintain constant pH. Samples were then centrifuged at 13,000×g for 10 min. 550 µl of supernatant were retrieved in microcentrifuge tubes and 50 µl of 1 mM TSP (trimethylsilyl propionic acid: 269913-1 g, lot number MBBB0475V, Sigma-Aldrich Chemie GmbH, Germany) were added to be used as an external reference.

2.7.2. ¹H NMR analysis

550 µl of samples were transferred in 5 mm- NMR tubes and analyzed by ¹H NMR spectroscopy on a 500 MHz Bruker Avance spectrometer. Solvent suppression of residual water signal was achieved by using the NOESYPRESAT or Carr-Purcell-Meiboom-Gill (CPMG) pulse sequences, for urine or serum samples respectively. Water proton resonance was irradiated during the relaxation decay (1.5 s) and mixing time (0.1sec). ¹H NMR spectrum of each sample was collected using 64 scans containing 54,832 data points at a spectral width of 10330,578 Hz with an acquisition time of 2.65 s and a relaxation delay of 3.0 s.

2.8. NMR spectral data processing and multivariate analysis

The MestRe Nova 5.2.0 software (Mestre Lab Research, Santiago de Compostela, Spain) was used for phase (Auto-Metabonomics) and baseline (Full Auto - Whittaker smoother) corrections of all ¹H

NMR spectra. Chemical shifts were referenced to TSP (singlet resonance arbitrarily placed at 0.0 ppm) and spectra were normalized to TSP and binned. Spectrum over the ranged 0.08–10.0 ppm was divided into subregions of equal width (0.04 ppm) and the area under the curve of each of the 248 spectral subregions was integrated and converted to ASCII format. Output ASCII data were next exported to Microsoft Excel (Microsoft Office, 2003). The regions corresponding to residual water and urea resonances (4, 50–5,00; 5,50–6,00 respectively) were excluded from the analysis to suppress the residual water signal and to remove the urea signal that undergoes annoying diurnal variations. Each integrated subregion was then normalized to the total spectrum area.

The resulting data set was then exported to SIMCA-P+ 12.0 software (Umetrics AB, Sweden) for multivariate data analysis. Principal component analysis (PCA) supplies two types of graphs which are a simplified overview of a complex set of data. In the “scores plot”, each point corresponds to one observation, meaning the NMR spectrum of a sample. This simplified 2-D view of the dataset allows a quick identification of potential gathering or separations between groups. The second plot is called a “loadings plot” and highlights what variables (metabolites) are responsible for the discriminations between groups (each point corresponds to the mean chemical shift of a particular spectral sub region of 0.04 ppm width, and consequently to the corresponding urine metabolites). These variables are finally annotated from a database to identify the corresponding metabolites.

2.9. Statistical analysis

The physiological and clinical chemistry data obtained from studies were expressed as mean ± standard deviations. Then, Wilcoxon rank-sum tests (WRS) and Welch Two Sample *t*-test were used to evaluate the differences between control and intoxicated groups. WRS were also used to determine which identified metabolites were significantly different between groups. *p*-values lower than 0.05 were considered to indicate statistical significance.

3. Results

A pilot dose-escalating study was conducted in order to select the most appropriate doses to be used in the subsequent toxicology study on AAI and the AAI/AAIL. Results are detailed hereafter.

3.1. Respective biological, metabonomic and histological results after AAI versus AAI+AAIL exposure

Biological parameters measured throughout the study showed that food intake and body weight were rapidly decreased after dosing (See supplementary data). These effects were dependent on the tested compound and the dose, with a decreased toxicity gradient from AAI+AAIL to AAI and from the high to low dose. Polyuria was also observed (data not shown). In addition, BUN and SCr levels increased after dosing (See supplementary data). Serum levels of albumin, total protein and uric acid did not change by the exposure to the tested compounds (data not shown).

The superposition of ¹H NMR urine spectra allowed a quick overview of urine metabolic changes after dosing AA. As shown in Fig. 1, exposure to AAI (a) or AAI+AAIL (b) induced some increases in signal intensities corresponding to lactate, alanine, acetate, taurine, betaine and glucose over time, whereas those corresponding to alpha-ketoglutarate, creatinine, hippurate were lowered. Moreover, in both groups, an increase in the spectral region close to 1.00 ppm was noticed over time. This region could correspond to the presence of some amino acids (leucine, valine) at 48 h. All these metabolic changes were observed in the urine of rats exposed

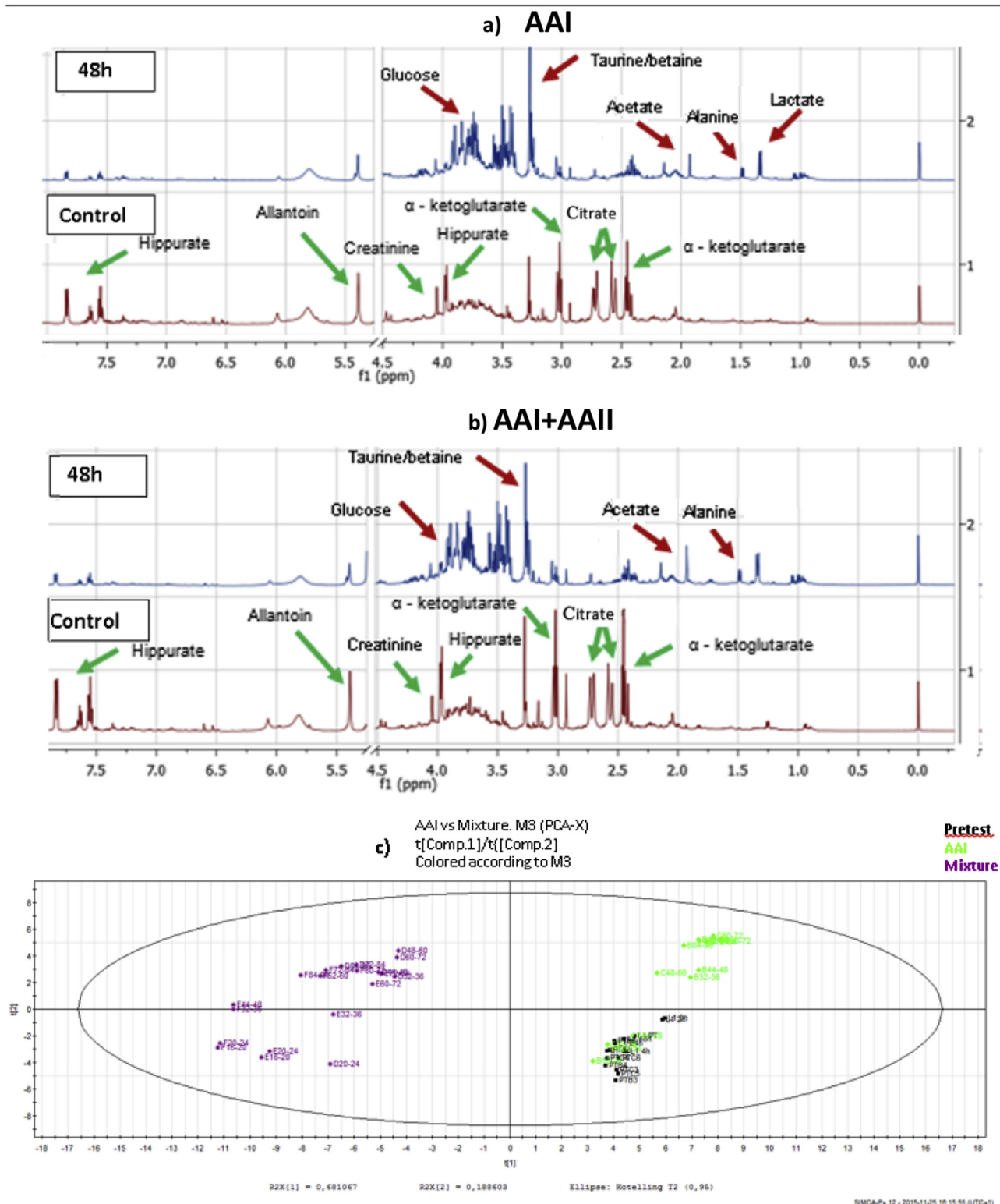


Fig. 1. Comparison of metabonomic profiles between AA and control groups. Spectra obtained by ^1H NMR analysis of control & 48 h post-dose urine sample collected from rats injected with the 75 mg/kg of AAI (a) or 50 mg/kg of AAI+AAII (b) are superimposed for a visual comparison of urinary changes. Several changes are observed between the control sample and the post-dose sample. Peaks corresponding to hippurate (3.97 + 7.55; 7.61; 7.84 ppm), allantoin (5.38 ppm), creatinine (4.05 ppm), α -ketoglutarate (3.01; 2.44 ppm) and citrate (2.52; 2.65)) are higher in control samples. On the contrary peaks of lactate (1.32 ppm), alanine (1.48 ppm), taurine/betaine (3.25/3.27), glucose region and acetate (1.92 ppm) increased. Spectra from 0.00 to 8.00 ppm. Water region (4.5–5.25 ppm) was cut. In the scores plot (c), urine samples from the 3 different groups are compared: In black are those collected from the control rats. Samples colored in green and violet correspond to rats injected with AAI and AAI+AAII, respectively.

either to AAI or AAI+AAII except in the animal exposed to the low dose of AAI. In this case, no urinary change was observed by peak-to-peak comparison. The scores plot generated by the multivariate analysis allowed us to clearly visualize gathering or separations between the different study groups but also to identify those metabolites which are responsible for such gathering or separations. As shown in Fig. 1c, the scores plot obtained by comparing urine samples from controls versus intoxicated groups (AAI vs AAI+AAII) reveals a clear discrimination between metabolomic profiles obtained with AAI and AAI+AAII. The AAI+AAII group is more distant than the AAI group, suggesting a more pronounced toxic effect. Some samples from the AAI group are co-located with samples from the control group, suggesting a delayed onset of the toxicity in this AAI group. In parallel, the lesions of tubular and interstitial structures consecutive to AA exposure were assessed on the basis of morphological criteria.

As shown in Fig. 2 (A–F), at 96 h after 50 mg/kg AAI exposure of rats, no morphological lesion was observed in the tubular compartment. However, some inflammatory cells were observed in the vessels (A–B). Rats treated with higher doses of AAI (75 and 100 mg/kg), proximal tubules exhibited damages such as loss of brush border, cell necrosis or focal epithelial desquamation, especially in the outer stripe of the outer medulla (OSOM) with a fairly well preserved cortex area at dose of 75 mg/kg (C–D). In contrast, cortex area also showed these pathological changes at the dose of 100 mg/kg. At these doses, numerous inflammatory cells were also present in the vessels (E–F).

Regarding the use of the mixture AAI+AAII (Fig. 3A–F), acute tubular necrosis was already present in proximal tubules, mostly in the OSOM after a dose of 50 mg/kg (A–B). The degree of severity of tubular necrosis was extended to the cortex area after higher doses (75 and 100 mg/kg) of the mixture AAI+AAII. In addition, in the interstitium, AA exposure induced an increase in interstitial cell density (C–F). Sign of proteinuria was revealed by the presence of PAS-positive casts in the lumen of some collecting ducts (H).

3.2. Confirmation of the stronger long-term toxicity of the mixture AAI+AAII

Based on these results, a second study was designed to further investigate the respective effects of AAI alone versus AAI+AAII. Twelve rats were subcutaneously injected with 100 mg/kg of AAI ($n = 6$) or 75 mg/kg of AAI+AAII ($n = 6$). Control rats were also used in this study ($n = 4$). In order to identify a possible reversibility of toxicity, the study design was prolonged to 192 h. Animals received one single dose of the tested compound and urine and blood samples were collected over a period of 7 days. All rats from the AAI group survived until the scheduled euthanasia time. In AAI+AAII group, one animal was prematurely euthanized after 120 h and another after 144 h for ethical reason (excessive loss of body weight). Results obtained in this additional study confirm the higher toxicity of AAI+AAII. Compared to control group, the food intake and the body weight significantly decreased after exposure to AAI and were more drastically reduced after injection of the AAI+AAII (Fig. 4 a,b). Increases in BUN and SCr levels were also significantly different compared to control group and were more pronounced in rats intoxicated with AAI+AAII as indicated (Fig. 4 c,d).

Histologically, a minor population of atrophic tubules was present 192 h after AAI exposure, mostly in the OSOM along with a chronic inflammation (Fig. 2G and H). After exposure to AAI+AAII, proteinuria was sustained at 192 h after exposure. As illustrated in Fig. 3 (G,H), the renal parenchyma was characterized by tubulointerstitial alterations, as attested by the presence of atrophic tubules and chronic inflammation.

3.3. Short-term toxicity of AAII alone

In a third study, the protocol used for the pilot study was applied to test the toxicity of AAII alone at several doses as compared to a control group ($n = 4$ for each group). Because of the dramatic

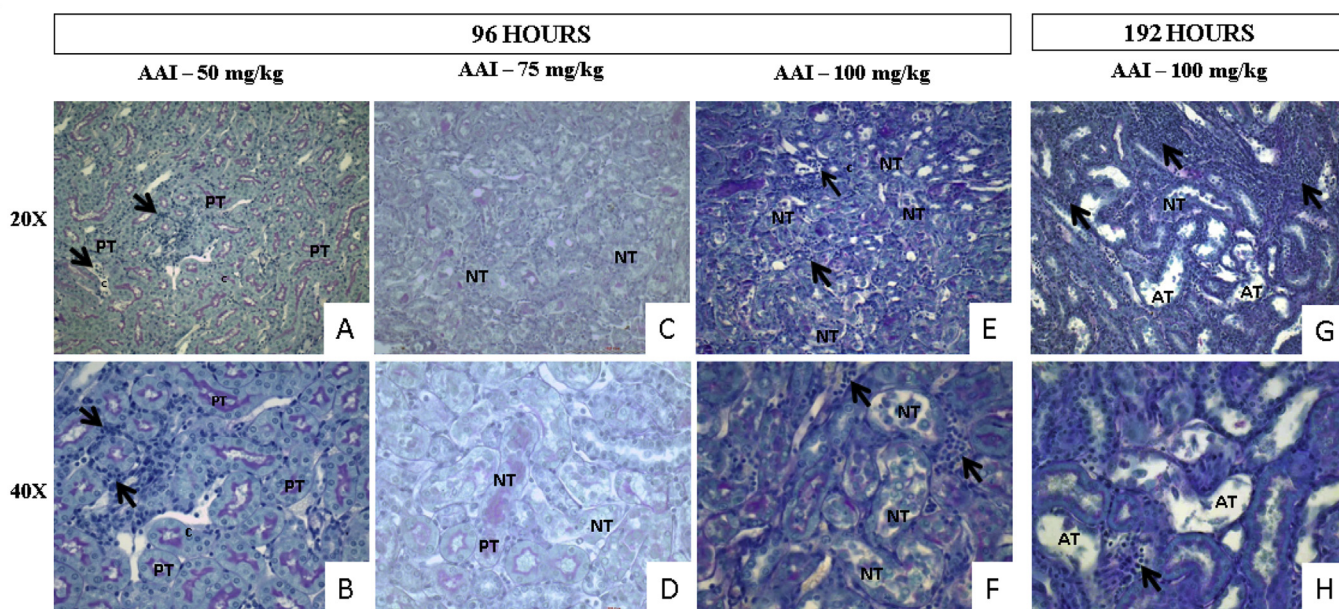


Fig. 2. Representative photomicrographs (original magnification A,C,E,G $\times 20$ – B,D,F,H $\times 40$) illustrating tubular and interstitial injuries in AAI 50 mg/kg (A,B), AAI 75 mg/kg (C,D) and AAI 100 mg/kg (E,F)-intoxicated rats at 96 h. Necrotic tubules (NT) with cell debris in tubular lumens were visible in AAI 75 mg/kg and AAI 100 mg/kg-treated rats and inflammatory cells (arrow) are visible in all three groups. At 192 h after AAI 100 mg/kg intoxication, few atrophic tubules (AT) were present, mostly in the OSOM area. This was associated with a significant interstitial infiltration by inflammatory cells (arrows) (G,H). PT: Proximal Tubule.

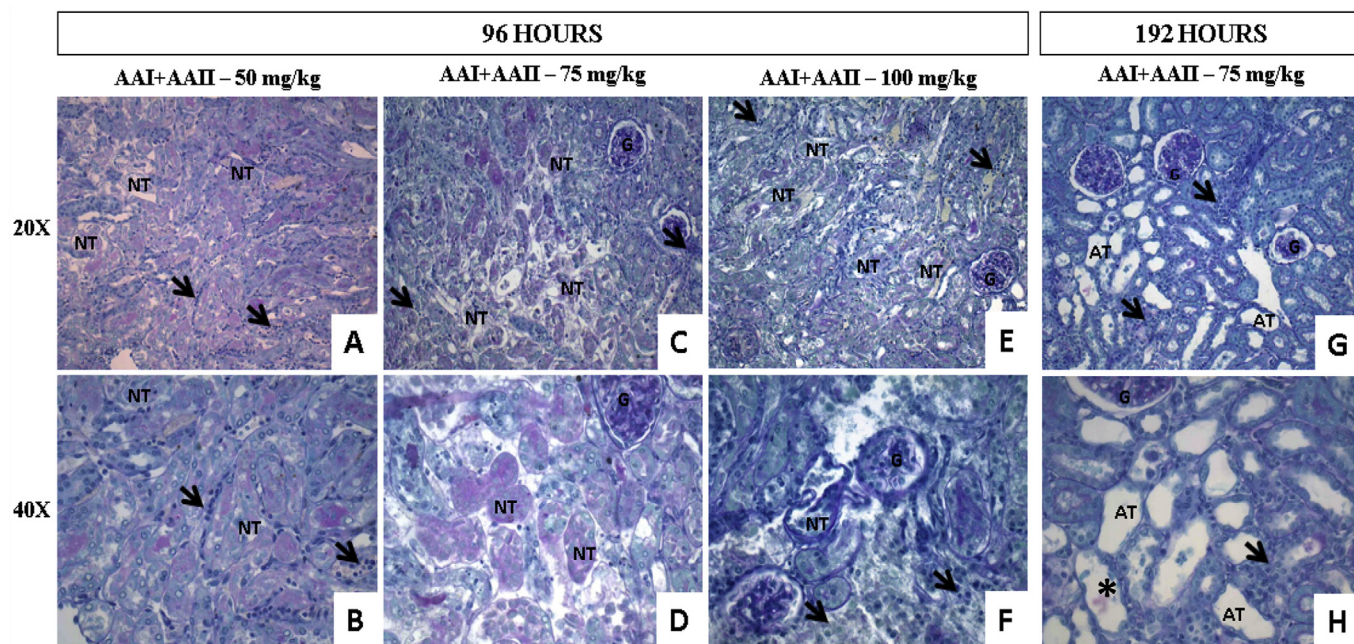


Fig. 3. Representative photomicrographs (original magnification A,C,E,G $\times 20$ – B,D,F,H $\times 40$) illustrating tubular and interstitial injuries in AAI+II 50 mg/kg (A,B), AAI+II 75 mg/kg (C,D) and AAI+II 100 mg/kg (E,F)-intoxicated rats at 96 h. Necrotic tubules (NT) with cell debris in tubular lumens were already visible in AAI+II 50 mg/kg (A,B) and was greatly extended at AAI+II 75 mg/kg (C,D) and 100 mg/kg-treated rats (E,F). These tubular alterations were associated with an increase in inflammatory cells (arrow) in all three groups. At 192 h after AAI+II 75 mg/kg-intoxicated rats, atrophic tubules (AT) were present in the OSOM and also in cortex areas. This was associated with a significant increase in inflammatory cells infiltrate (arrows) (G-H). G: glomerulus. *PAS-positive casts.

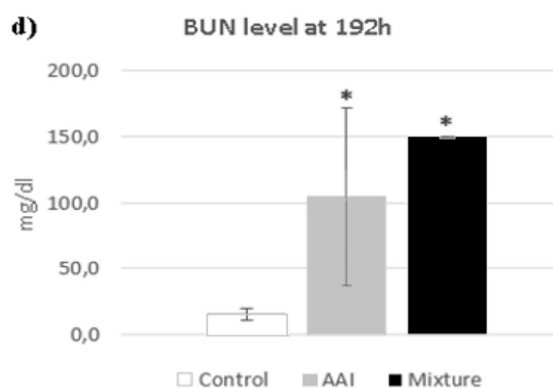
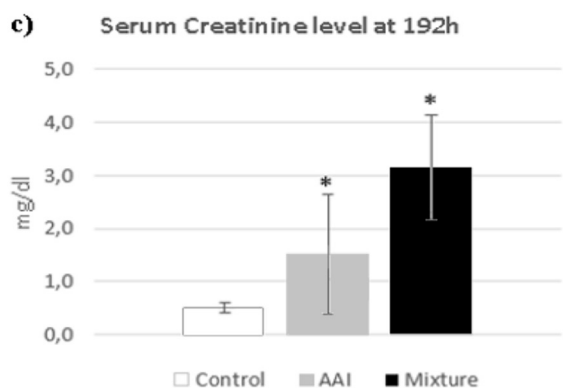
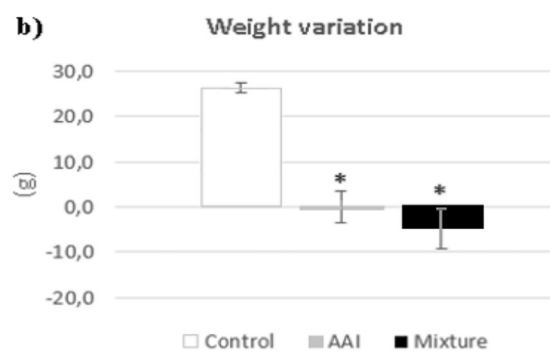
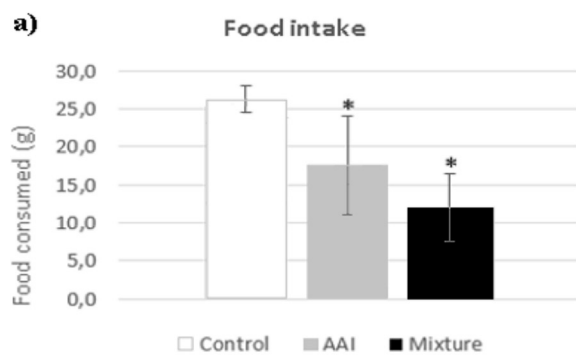


Fig. 4. Comparison of food intake, weight variation, BUN and SCr in relation with the toxic agent. As seen previously, food intake and weight variation decreased whereas BUN and SCr. increased after injection of AAI (100 mg/kg). These changes were more severely affected after injection of the AAI+AAII (75 mg/kg). * indicates statistically different from control group (p-value < 0, 05; t-test).

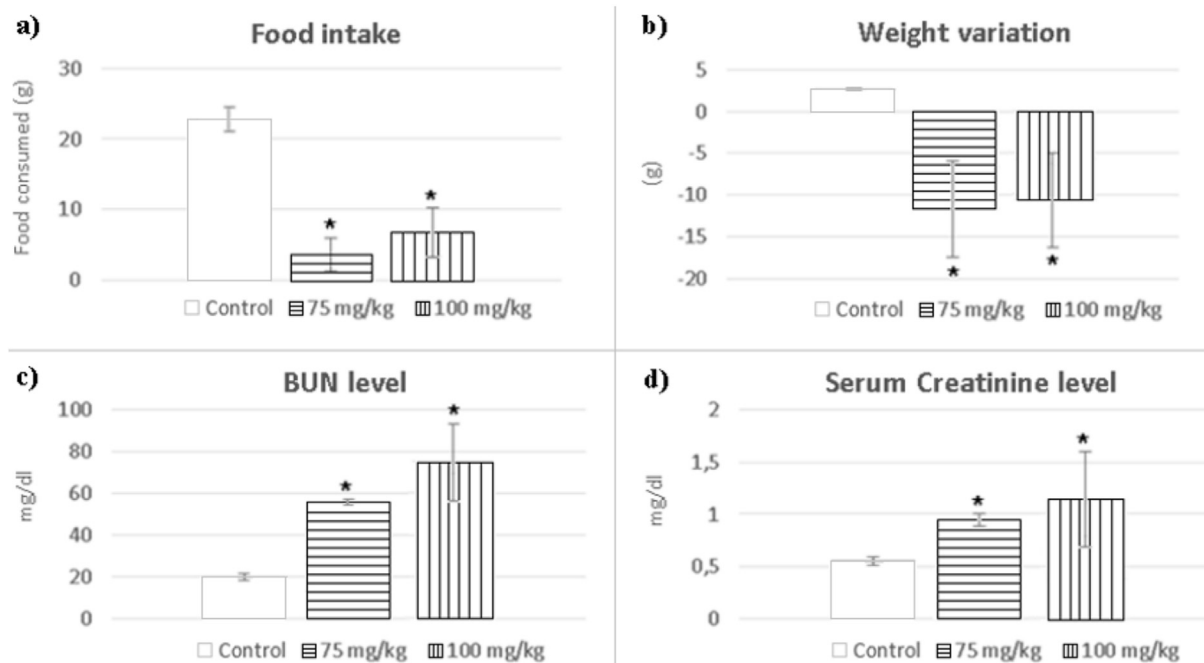


Fig. 5. Comparison of food intake, body weight, BUN and Scr levels after AAIL exposure. As seen previously with AAI and AAI+AAIL, food intake and body weight decrease after injection of AAIL whereas BUN and Scr increased. These effects seem to be more drastic for AAIL than for AAI and the AAI+AAIL. * indicates statistically different from control group (p-value < 0, 05; WRS test).

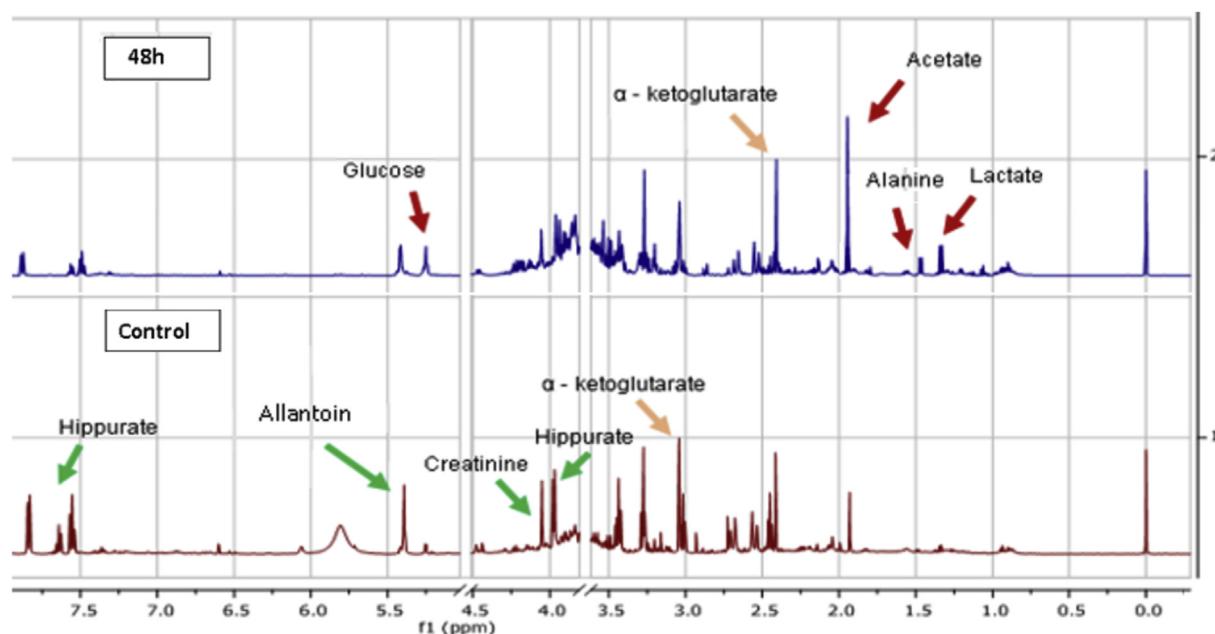


Fig. 6. Metabonomic profiles of urine samples from rats exposed to AAI, AAI+AAIL or AAIL versus control rats. Spectra obtained by ^1H NMR analysis of control and post-dose urine samples collected from rats receiving 75 mg/kg of AAIL are superimposed for a visual comparison of urinary changes. Several changes are observed between the control sample and the post-dose samples (from 24 h to 48 h after injection): Peaks corresponding to hippurate (3.97 + 7.55; 7.61; 7.84 ppm), allantoin (5.38 ppm) and creatinine (4.05 ppm) are higher in pretest sample. On the contrary peaks of lactate (1.32 ppm), alanine (1.48 ppm), Glucose region, and acetate (1.92 ppm) increased. Spectra from 0.00 to 8.00 ppm, water region (4.5–5.25 ppm) and PEG peaks (3.65–3.73 ppm) were removed prior to the analysis.

weight loss observed in rats exposed to AAIL, the study protocol was prematurely ended: 3 rats had to be euthanized after 48 h and the remaining animals after 72 h. The results (food intake, weight gain and biological parameters) are presented in Fig. 5.

Significantly decreased urinary levels of creatinine, hippurate, allantoin, α -ketoglutarate were found in the metabonomic profiles,

whereas glucose, acetate, alanine and lactate levels tended to increase after injection of AAIL (Fig. 6).

In some rats, a dramatic but not significant increase in urinary acetate level was observed as well as peaks corresponding to amino acids. As illustrated in Fig. 7 (A–H), rats treated with AAIL at 75 and 100 mg/kg exhibited similar lesions in tubular and interstitial

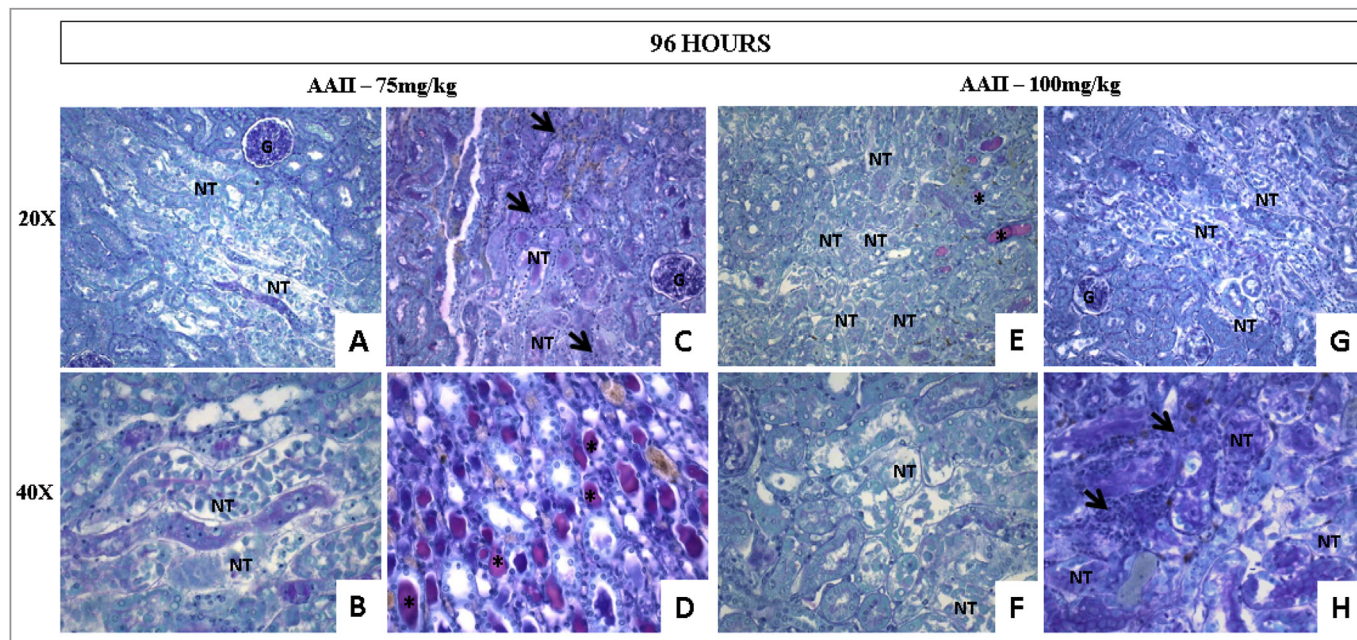


Fig. 7. Representative photomicrographs (original magnification A,C,E,G $\times 200$ – B,D,F,H $\times 400$) illustrating tubular and interstitial injuries in AAI 75 mg/kg (A–D), AAI 100 mg/kg (E–H) -intoxicated rats at 96 h. Significant proportion of necrotic tubules (NT) with cell debris in tubular lumens were present in AAI 75 mg/kg (A–D). This was even greatly increased at AAI 100 mg/kg-treated rats (E–H). These tubular alterations were associated with an increase of inflammatory cells (arrow) in both doses (C,H). Sign of proteinuria was revealed by the presence of PAS-positive casts in the lumen of some collecting ducts (*) (D, E).

structures than rats treated with the mixture of AAI+AAII. Indeed, acute tubular necrosis was present in proximal tubules from the cortex and OSOM areas (A–B). The degree of severity of tubular necrosis was even enhanced at 100 mg/kg of AAI (E–H). In addition, in the interstitium, AAI exposure also induced an increase in interstitial cell density (Fig. 7 C, H). In parallel, sign of proteinuria was revealed by the presence of PAS-positive casts in the lumen of some collecting ducts (Fig. 7 D, E).

4. Discussion

Both genomic and proteomic approaches have already been applied to investigate the cellular mechanisms of AA toxicity and highlighted characteristic patterns of AA exposure, demonstrating among others specific mutation in p53, the suppressor tumor gene, and urinary excretion of some low MW proteins such as alpha-1-microglobuline (Grollman et al., 2007; Rucevic et al., 2012; Slade et al., 2009). Specific AA-DNA adducts formed during the biotransformation of AA are also proposed as histological biomarkers of prior exposure to AA (Jelakovic et al., 2012). Although

these biomarkers are useful to understand the toxic mode of action of AA, their identification/detection still requires heavy analytical methods such as tissue collection, DNA isolation, fragmentation, and amplification, hybridization to oligonucleotides (Grollman et al., 2007; Rucevic et al., 2012; Dong et al., 2006). By comparison, the metabonomic approach offers many advantages: samples collection and preparation are fast and simple and metabonomic biomarkers are most often detected at early stages of the pathology, making of this method a powerful predictive tool (Wishart, 2006). In the context of intoxications due to AAs-exposure, several authors have shown the diagnostic, prognostic and predictive power of this metabonomic tool either in animal models (Hu et al., 2017; Chen et al., 2016; Zhao et al., 2015a; Zhao et al., 2015b) or in humans (Mantle et al., 2011; Duquesne et al., 2012).

In the present study conducted in rats, the metabonomic tool was used to evaluate and compare the respective toxic responses to either AAI or AAII alone or to the mixture (AAI+AAII) towards the proximal tubule. Our main results identified significant changes in metabolites, whose levels were either increased or decreased, reflecting functional cell impairments which could be considered

Table 2
Respective decreased and increased metabolites after exposure to AAI, AAII or AAI+AAII compared to control group. Significant metabolites appear in bold.

Group	Decreased metabolites (p-value)	Fold-changes	Increased metabolites (p-value)	Fold-changes
AAI	Citrate (0.004)	0,39	Glucose (0,122)	1,28
	Alpha-ketoglutarate (0.04)	0,65	Glycine (0,125)	1,44
	Succinate (0,33)	0,78	Lactate (0,329)	1,20
	Hippurate (0,537)	0,86	Creatinine (1)	1,02
	Citrate (0.004)	0,31	Glucose (0.004)	1,98
AAI+AAII	Alpha-ketoglutarate (0.006)	0,40	Glycine (0.004)	2,10
	Succinate (0.02)	0,61	Lactate ((0.004)	1,45
	Hippurate (0,429)	0,94	Creatinine (0.004)	1,29
	Citrate (0.004)	0,15	Glucose (0.002)	1,62
	Alpha-ketoglutarate (0.004)	0,26	Glycine (0.002)	1,47
AAII	Succinate (0.01)	0,37	Lactate (0,699)	1,13
	Creatinine ((0.005)	0,44		
	Hippurate (0.002)	0,23		

as early biomarkers of AA toxicity (Table 2).

The exposure to AA causes a higher glycosuria. After glomerular filtration, glucose is massively reabsorbed by two different types of membrane transporters localized in the different parts of the proximal tubular epithelium. Within the brush border, two active sodium glucose co-transporters SGLT2 in S1 and SGLT1 in S3 segment reabsorb 90% and 10% of the filtered glucose fraction, respectively. Then, its way back to the bloodstream is facilitated by two basolateral membrane glucose transporters, GLUT2 and GLUT1 in the S1 and S3 segments, respectively (Rahmoune et al., 2005). As observed histologically, AA toxicity is marked by a dramatic loss of the brush border suggesting that the massive glycosuria observed after AA intoxication, reflects a defect of reabsorptive capacity of glucose by transport systems due to the disappearance of the apical membrane. The reduction in the Krebs cycle activity as evidenced by the reduced levels of its intermediaries in urine samples (succinate, citrate, alpha-ketoglutarate) after exposure to AA is most likely consecutive to this poor availability of glucose, normally consumed by the glycolysis to produce pyruvate that supplies the Krebs cycle. However, it is well demonstrated that mitochondrial stress occurs during AA exposure (Hsin et al., 2006). Given that mitochondria are the place for Krebs cycle and are quite abundant in the brush border of the proximal tubules, the deficiency in the Krebs cycle activity may be seen as a mitochondrial dysfunction.

Hippurate is synthesized by the conjugation of glycine and benzoate in the kidney but also in the liver and in the intestine (Poon and Pang, 1995; Strahl and Barr, 1971). As previously shown by Deguchi et al. in 2005, circulating hippurate molecules are mostly uptaken by the organic anion transporter 1 in rats (rOat1) located in the basolateral membrane of kidney. Hence, active tubular secretion is the major route to eliminate hippurate. Consequently, the renal clearance of endogenous hippurate is proposed as a useful indicator of changes in renal secretion during chronic renal failure associated with reduced levels of OAT proteins (Deguchi et al., 2005). Thus, the decreased hippurate secretion observed in our study could be due to a loss of OAT1 transporters in the damaged basolateral membrane after AA exposure. Moreover, as AA presents a chemical structure common to known OAT substrates, it was already suggested that AA and hippurate use the same transporter to enter the proximal tubule cell (Dickman et al., 2011; Bakhia et al., 2009; Babu et al., 2010). In addition, the protective effect of probenecid, an inhibitor of organic acid transporters towards the proximal tubular cells in an AAN mouse model has been demonstrated (Baudoux et al., 2012). Thus, these additional observations support the competitive transport between hippurate and AA which would jeopardize the renal secretion of hippurate.

Elevated urine concentrations of acetate and lactate are markers

Table 4

Semi-quantitative summary of respective morphological abnormalities observed after exposure to AAI, AAI+AAII or AAII.

Time-points	Dose	Renal lesions	AAI	AAI+AAII	AAII
96 h	50 mg/kg	Cortex	–	–	X
		OSOM	–	+ (prot.)	
	75 mg/kg	Cortex	–	+	+
		OSOM	+	++ (prot.)	++ (prot.)
	100 mg/kg	Cortex	+	++	++
		OSOM	++	++ (prot.)	++ (prot.)
192 h	75 mg/kg	Proteic casts	++	X	X
		Atrophic tubules	+	X	X
	100 mg/kg	Proteic casts	X	+++	X
		Atrophic tubules	X	++	X

of proximal tubular metabolism injury and acute tubular necrosis (Hauet et al., 2000). Although the highest levels of lactate are found in muscles, lactate production occurs in most tissues of the human body. It is chiefly cleared by the liver and converted to glucose through the Cori cycle. In aerobic conditions, lactate production is bypassed by pyruvate which then enters the Krebs cycle. Under anaerobic conditions, lactate is produced during glycolysis and serves for gluconeogenesis. Thus, the increase of urine lactate levels associated to the lack of glucose availability could be interpreted as the onset of anaerobic pathway as energy source.

Creatinine, a nitrogenous compound, is the breakdown product of creatine phosphate metabolism in muscle. It is produced at constant rate by the body and released in the bloodstream to finally undergo renal glomerular filtration and, to a lesser extent, proximal tubular secretion. When glomerular filtration is reduced, creatinine levels rise in blood and decrease in urine (Klawitter et al., 2010). Therefore, the decrease in urine creatinine levels together with its increase in serum, as observed in AA rats, may reflect a reduced glomerular filtration but also a secretion defect by PTEC.





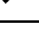
Histological analyses of kidney tissue samples highlighted that AA exposure causes massive brush border loss, tubular necrosis, proteinuria and increased inflammatory cells. Interestingly, these observations are consistent with the biological interpretation of the identified metabolites (Table 3).

Moreover, the morphological alterations were more pronounced in rats exposed to AAI+AAII or AAII alone than those only exposed to AAI and the dose-dependent effects were also histologically observed, in parallel with our metabolomic findings (Table 4).

To conclude, combining our urinary metabolomic data to biochemical and histological results, we propose a cascade of early

Table 3

Summary of metabolomic and histological results.

Metabolites	Urinary levels	Markers of	Histological observation
Succinate Citrate Alpha-ketoglutarate Creatinine		Krebs cycle deficiency; mitochondrial dysfunction; lack of energy (glucose)	Brush border loss
Hippurate		Altered filtration/secretion balance	Brush border loss
Glucose		Tubular secretion defect	Brush border loss
Lactate		Tubular reabsorption defect	Brush border loss
		Necrosis, anaerobic metabolism	Tubular necrosis

physiopathological events consecutive to AA exposure. Renal tubular cells, main targets of AA, are affected by an apoptotic wave leading, among others, to the loss of apical-basolateral polarity. As explained before, tubular cell apoptosis/necrosis which is reflected by increased levels of lactate and acetate, affects the reabsorption/secretion processes, leading to glycosuria and a decreased excretion of hippurate. A defect in glucose reabsorption associated with a reduced food consumption (observed in most of our AA-exposed animals) causes a shift in energy metabolism. Lactate, therefore, appears to be the most available energy source through the Cori cycle, which involves neoglucogenesis and anaerobic glycolysis steps.

Acknowledgements

Professor L. Vander Elst from the Department of General, Organic and Biomedical chemistry at UMONS is kindly acknowledged for her support in the NMR analysis.

This research did not receive any specific grant from funding agencies in the public, commercial or not-for-profit sectors.

Transparency document

Transparency document related to this article can be found online at <http://dx.doi.org/10.1016/j.fct.2017.07.015>.

Appendix A. Supplementary data

Supplementary data related to this article can be found at <http://dx.doi.org/10.1016/j.fct.2017.07.015>.

References

- Babu, E., Takeda, M., Nishida, R., Noshiro-Kofuji, R., Yoshida, M., Ueda, S., Fukutomi, T., Anzai, N., Endou, H., 2010. Interactions of human organic anion transporters with aristolochic acids. *J. Pharmacol. Sci.* 113, 192–196. <http://dx.doi.org/10.1254/jphs.093395C>.
- Bakhiya, N., Arlt, V.M., Bahn, A., Burckhardt, G., Phillips, D.H., Glatt, H., 2009. Molecular evidence for an involvement of organic anion transporters (OATs) in aristolochic acid nephropathy. *Toxicology* 264, 74–79. <http://dx.doi.org/10.1016/j.tox.2009.07.014>.
- Baudoux, T.E., Pozdzik, A.A., Arlt, V.M., De Prez, E.G., Antoine, M.H., Quellard, N., Goujon, J.M., Nortier, J.L., 2012. Probenecid prevents acute tubular necrosis in a mouse model of aristolochic acid nephropathy. *Kidney Int.* 10, 1105–1113. <http://dx.doi.org/10.1038/ki.2012.264>.
- Chen, C.H., Dickman, K.G., Moriya, M., Zavadil, J., Sidorenko, V.S., Edwards, K.L., et al., 2012. Aristolochic acid-associated urothelial cancer in Taiwan. *Proc. Nat. Acad. Sci.* 109, 8241–8246. <http://dx.doi.org/10.1073/pnas.1119920109>.
- Chen, H., Cao, G., Chen, D.Q., Wang, M., Vaziri, N.D., Zhang, Z.H., Mao, J.R., Bai, X., Zhao, Y.Y., 2016 Dec. Metabolomics insights into activated redox signaling and lipid metabolism dysfunction in chronic kidney disease progression. *Redox Biol.* 10, 168–178. <http://dx.doi.org/10.1016/j.redox.2016.09.014>.
- Commission of the Ministry of Public Health, 2000. *Pharmacopoeia (Part I)*. Chemical Industry Press, Beijing, pp. 31, 39, 41, 114, 154.
- Cosyns, J.P., Jadoul, M., Squifflet, J.P., De Plaen, J.F., Ferluga, D., van Ypersele de, S.C., 1994 Jun. Chinese herbs nephropathy: a clue to Balkan endemic nephropathy? *Kidney Int.* 45 (6), 1680–1688. <http://dx.doi.org/10.1038/ki.1994.220>.
- Cosyns, J.P., Jadoul, M., Squifflet, J.P., Wese, F.X., van Ypersele de, S.C., 1999 Jun. Urothelial lesions in Chinese herb nephropathy. *Am. J. Kidney Dis.* 33 (6), 1011–1017. [http://dx.doi.org/10.1016/S0272-6386\(99\)70136-8](http://dx.doi.org/10.1016/S0272-6386(99)70136-8).
- Debelle, F.D., Nortier, J., De Prez, E.G., Garbar, C.H., Vienne, A.R., Salmon, I.J., Deschodt-Lanckman, M.M., Vanherweghem, J.-L., 2002. Aristolochic acids induce chronic renal failure with interstitial fibrosis in salt-depleted rats. *J. Am. Soc. Nephrol.* 13, 431–436.
- Debelle, F.D., Vanherweghem, J.L., Nortier, J.L., 2008 Jul. Aristolochic acid nephropathy: a worldwide problem. *Kidney Int.* 74 (2), 158–169. <http://dx.doi.org/10.1038/ki.2008.129>.
- Deguchi, T., Takemoto, M., Uehara, N., Lindup, W.E., Suenaga, A., Otagiri, 2005. Renal clearance of endogenous hippurate correlates with expression levels of renal organic anion transporters in uremic rats. *JPET* 314, 932–938. <http://dx.doi.org/10.1124/jpet.105.085613>.
- Dickman, K.G., Sweet, D.H., Bonala, R., Ray, T., Wu, A., 2011. Physiological and molecular characterization of aristolochic acid transport by the kidney. *JPET* 338, 588–597. <http://dx.doi.org/10.1124/jpet.111.180984>.
- Dong, H., Suzuki, N., Torres, M.C., Bonala, R.R., Johnson, F., Grollman, A.P., Shibutani, S., 2006. Quantitative determination of Aristolochic acid derived DNA adducts in rats using 32-postlabelling/polyacrylamide electrophoresis analysis. *Drug Meta Dispos* 34 (No.7). <http://dx.doi.org/10.1124/dmd.105.008706>.
- Duquesne, M., Goossens, C., Dika, Z., Conotte, R., Nortier, J., Jelaković, B., Colet, J.M., 2012. "Metabonomics: on the road to detect diagnostic biomarkers in endemic (Balkan) nephropathy. Evaluation in a Retrospective Pilot Project. *J. Cancer Sci. Ther.* S18, 1–9. <http://dx.doi.org/10.4172/1948-5956.S18-002>.
- Gökmen, M.R., Cosyns, J.P., Arlt, V.M., Stiborova, M., Phillips, D.H., Schmeiser, H.H., 2013. The epidemiology, diagnosis and management of aristolochic acid nephropathy: a narrative review. *Ann. Int. Med.* 158, 469–477. <http://dx.doi.org/10.7326/0003-4819-158-6-201303190-00006>.
- Grollman, A.P., Shibutani, S., Moriya, M., Miller, F., Wu, L., Moll, U., et al., 2007. Aristolochic acid and the etiology of endemic (Balkan) nephropathy. *Proc. Natl. Acad. Sci. U. S. A.* 104, 12129–12134. <http://dx.doi.org/10.1073/pnas.0701248104>.
- Hauet, T., Baumert, H., Gibelin, H., Hamuery, F., Goujon, J.M., Carretier, M., Eugene, M., 2000. Noninvasive monitoring of citrate, acetate, lactate and renal medullary osmolyte excretion in urine as biomarkers of exposure to ischemic reperfusion injury. *Cryobiology* 41, 280–291. <http://dx.doi.org/10.1006/cryo.2000.2291>.
- Hsin, Y.H., Cheng, C.H., Tzen, J.T.C., Wu, M.J., Shu, K.H., Chen, H.C., 2006. Effect of aristolochic acid on intracellular calcium concentration and its links with apoptosis in renal tubular cells. *Apoptosis* 11, 2167–2177. <http://dx.doi.org/10.1007/s10495-006-0289-0>.
- Hu, X., Shen, J., Pu, X., Zheng, N., Deng, Z., Zhang, Z., Li, H., 2017. Urinary time- or dose-dependent metabolic biomarkers of aristolochic acid-induced nephrotoxicity in rats. *Toxicol. Sci.* 156 (1), 123–132. <http://dx.doi.org/10.1093/toxsci/kfw244>.
- IARC, 2002. Some traditional herbal medicines, some mycotoxins, naphthalene and styrene. *IARC Monogr. Eval. Carcinog. Risks Hum.* 82, 1–556.
- Ivic, M., 1969. Etiology of endemic nephropathy. *Lijec. Vjesn.* 91, 273–281.
- Jelakovic, B., Karanovic, S., Vukovic-Lela, I., Miller, F., Edwards, K.L., Nikolic, et al., 2012. Aristolactam-DNA adducts are a biomarker of environmental exposure to aristolochic acid. *Kidney Int.* 81 (6), 559–567. <http://dx.doi.org/10.1038/ki.2011.371>.
- Klawitter, J., Haschke, M., Dingmann, C., Klawitter, J., Leibfritz, D., Christians, U., 2010 Aug. Toxicodynamic effects of ciclosporin are reflected by metabolite profiles in the urine of healthy individuals after a single dose. *Br. J. Clin. Pharmacol.* 70 (2), 241–251. <http://dx.doi.org/10.1111/j.1365-2125.2010.03689.x>.
- Lebeau, C., Debelle, F.D., Arlt, V.M., Pozdzik, A., De Prez, E.G., Phillips, D.H., Deschodt-Lanckman, M.M., Vanherweghem, J.-L., Nortier, J.L., 2005. Early proximal tubule injury in experimental Aristolochic acid nephropathy: functional and histological studies. *Nephrol. Dial. Transpl.* 20, 2321–2332. <http://dx.doi.org/10.1093/ndt/gfi042>.
- Nortier, J.L., Martinez, M.C., Schmeiser, H.H., et al., 2000 Jun. Urothelial carcinoma associated with the use of Chinese herb (Aristolochia fangchi). *N. Engl. J. Med.* 342 (23), 1686–1692. <http://dx.doi.org/10.1056/NEJM200006083422301>.
- Mantle, P.I., Modalca, M., Nicholls, A., Tatu, C., Tatu, D., Toncheva, D., 2011. Comparative (1)H NMR metabolomic urinalysis of people diagnosed with Balkan endemic nephropathy, and healthy subjects, in Romania and Bulgaria: a pilot study. *Toxins (Basel)* 3 (7), 815–833. <http://dx.doi.org/10.3390/toxins3070815>.
- Poon, K., Pang, K.S., 1995 Feb. Benzoic acid glycine conjugation in the isolated perfused rat kidney. *Drug Metab. Dispos.* 23 (2), 255–260.
- Rahmoune, H., Thompson, P.W., Ward, J.M., Smith, C.D., Hong, G., Brown, J., 2005 Dec. Glucose transporters in human renal proximal tubular cells isolated from the urine of patients with non-insulin-dependent diabetes. *Diabetes* 54.
- Rucevic, M., Rosenquist, T., Breen, L., Cao, L., Clifton, J., Hixson, D., Josic, D., 2012. Proteome alterations in response to aristolochic acids in experimental animal model. *J. Proteomics* 76, 79–90. <http://dx.doi.org/10.1016/j.jpro.2012.06.026>.
- Takako, Seto, Tomoko, Hamano, Hiroko, Shioda, Hisashi, Kamimura, 2002. Analysis of aristolochic I and II in Kampo medicine preparations. *J. health Sci.* 48 (5), 412–417. <http://dx.doi.org/10.1248/jhs.48.412>.
- Slade, N., Moll, U., Brdar, B., Zorić, A., Jelaković, B., 2009 April. p53 mutations as fingerprints for aristolochic acid – an environmental carcinogen in endemic (Balkan) nephropathy. *Mutat. Res.* 663 (1–2), 1–6. <http://dx.doi.org/10.1016/j.mrfmmm.2009.01.005>.
- Strahl, N.R., Barr, W.H., 1971 Feb. Intestinal drug absorption and metabolism. III. Glycine conjugation and accumulation of benzoic acid in rat intestinal tissue. *J. Pharm. Sci.* 60 (2), 278–281. <http://dx.doi.org/10.1002/jps.2600600227>.
- Vanhaelen, M., Vanhaelen-Fastre, R., But, P., Vanherweghem, J.L., 1994 Jan. Identification of aristolochic acid in Chinese herbs. *Lancet* 343 (8890), 174.
- Vanherweghem, J.L., Depierreux, M., Tielemans, C., et al., 1993. Rapidly progressive interstitial renal fibrosis in young women: association with slimming regimen including Chinese herbs. *Lancet* 13 (341), 387–391. [http://dx.doi.org/10.1016/0140-6736\(93\)92984-2](http://dx.doi.org/10.1016/0140-6736(93)92984-2).
- Wishart, D.S., 2006. Metabolomics in monitoring kidney transplants. *Curr. Opin. Nephrol. Hypertens.* 15, 637–642. <http://dx.doi.org/10.1097/01.mnh.0000247499.64291.52>.
- Yang, L., Su, T., Li, S.-M., Wang, X., Cai, S.-Q., Meng, L.-Q., et al., 2011. Aristolochic acid

- nephropathy: variation in presentation and prognosis. *Nephrol. Dial. Transpl.* <http://dx.doi.org/10.1093/ndt/gfr291>.
- Zhao, Y.Y., Tang, D.D., Chen, H., Mao, J.R., Bai, X., Cheng, X.H., Xiao, X.Y., 2015a. Urinary metabolomics and biomarkers of aristolochic acid nephrotoxicity by UPLC-QTOF/HDMS. *Bioanalysis* 7 (6), 685–700. <http://dx.doi.org/10.4155/bio.14.309>.
- Zhao, Y.Y., Wang, H.L., Cheng, X.L., Wei, F., Bai, X., Lin, R.C., Vaziri, N.D., 2015b. Metabolomics analysis reveals the association between lipid abnormalities and oxidative stress, inflammation, fibrosis, and Nrf2 dysfunction in aristolochic acid-induced nephropathy. *Sci. Rep.* 5, 12936. <http://dx.doi.org/10.1038/srep12936>.